Identification of Shallow Aquifer Zone Using Vertical Electrical Sounding (VES) Method with Schlumberger Array. Case Study: Universitas Indonesia

Y. Rustriandayani[1], AA. Valencia[1*], T. R. Fadia[1]

[1]Geophysics Study Program, Faculty of Mathematics and Natural Sciences, Universitas Indonesia, Depok, Indonesia

*Corresponding author: ayunda.aulia@ui.ac.id

Abstract

This study aims to identify shallow aquifers in Universitas Indonesia (UI). Fifteen Vertical Electrical Sounding (VES) surveys were conducted using the Schlumberger array. The VES method is used because it can penetrate a considerable depth where shallow aquifers may exist. In addition, this method can cover a significant area relatively quickly and minimise the effect of shallow lateral resistivity variation. The apparent resistivity from VES measurements was used in the curve-matching inversion to obtain the depth, thickness, and true resistivity of subsurface layers. The error from the inversion is kept below 5%. The result is then interpreted to determine lithology types, guided by the lithology log from boreholes and rock resistivity values from the literature. The lithology type in the study area consists of sand, silt and clay. Sand exhibits a resistivity range of less than 300 Ωm, interpreted as aquifers because they have higher porosity and permeability than silt and clay. Aquifers can be found at shallow depths (min 0.5 m) in almost all VES Lines, which are thicker towards the western part of the study area (up to 29.3 m). The information about the distribution of shallow aquifers is essential for decision-making regarding groundwater search and utilisation in the UI.

Keywords:*Vertical Electrical Sounding, VES, Aquifer, Schlumberger array, groundwater, Universitas Indonesia, UI*

1. Introduction

Universitas Indonesia (UI) is located in Depok, part of the Jakarta Metropolitan area. UI hosts thousands of students who need clean water to support their daily activities, mainly from the shallow groundwater (< 50 m). Therefore, it is essential to comprehend the aquifer potential (thickness and distribution) as a reference for decision-making of groundwater search and utilisation in UI. Geophysical techniques (i.e., Vertical Electrical Sounding) enable groundwater detection.

Vertical Electrical Sounding (VES) has been widely used for aquifer investigation in Indonesia and abroad (i.e., Hamzah et al., 2007; Coker, 2012; Aizebeokhai & Oyebanjo, 2013; Sholichin & Prayogo, 2019; Dzakiya et al., 2021; Muzakki et al., 2021; Wahab et al., 2021; Koesuma & Aldi, 2022; Maulana, 2022). For the UI area, the aquifer investigation was conducted by Ishaq (2008), which focused on deep aquifers (> 50 m). VES is a 1-D geoelectric method that determines subsurface layers' resistivity values and depths (Telford et al., 1990; Wahab et al., 2021). In addition, this method has a relatively considerable depth penetration and is cheap, making it suitable for groundwater exploration (Hadian et al., 2006; Syifaurrohman et al., 2018; Nuraini et al., 2022).

Therefore, this study aims to analyse the resistivity values of subsurface layers obtained by VES method to identify the thickness and distribution of shallow aquifers (<50 m) in the UI, conducted in several steps: (1) Fifteen VES measurements were run around UI. (2) VES data processing using IPI2Win software. (3) Interpretation of lithology types guided by the lithology log from boreholes and the literature. (4) Analyze the thickness and depth of aquifers in the study area.

2. Study Area

VES surveys were carried out around the UI (Figure 1). The distance between VES surveys from the closest to the furthest is 190 m (VES Lines 5 and 13) to 3750 m (VES Lines 2 and 13), respectively (Figure 1). The UI has a flat topography divided into the Northern Forest and Southern Campus areas. Two boreholes are available in the Campus area: (1) FE borehole is situated in the Faculty of Engineering (Lab Mekanika Tanah, 2008), whereas FN borehole is located in the Faculty of Nursing (Rizqulloh & Riyanto, 2020) (Figure 1). The boreholes provide the lithology log (depth vs lithology types) (Figure 2). The VES method and survey plan are explained in the following sections.

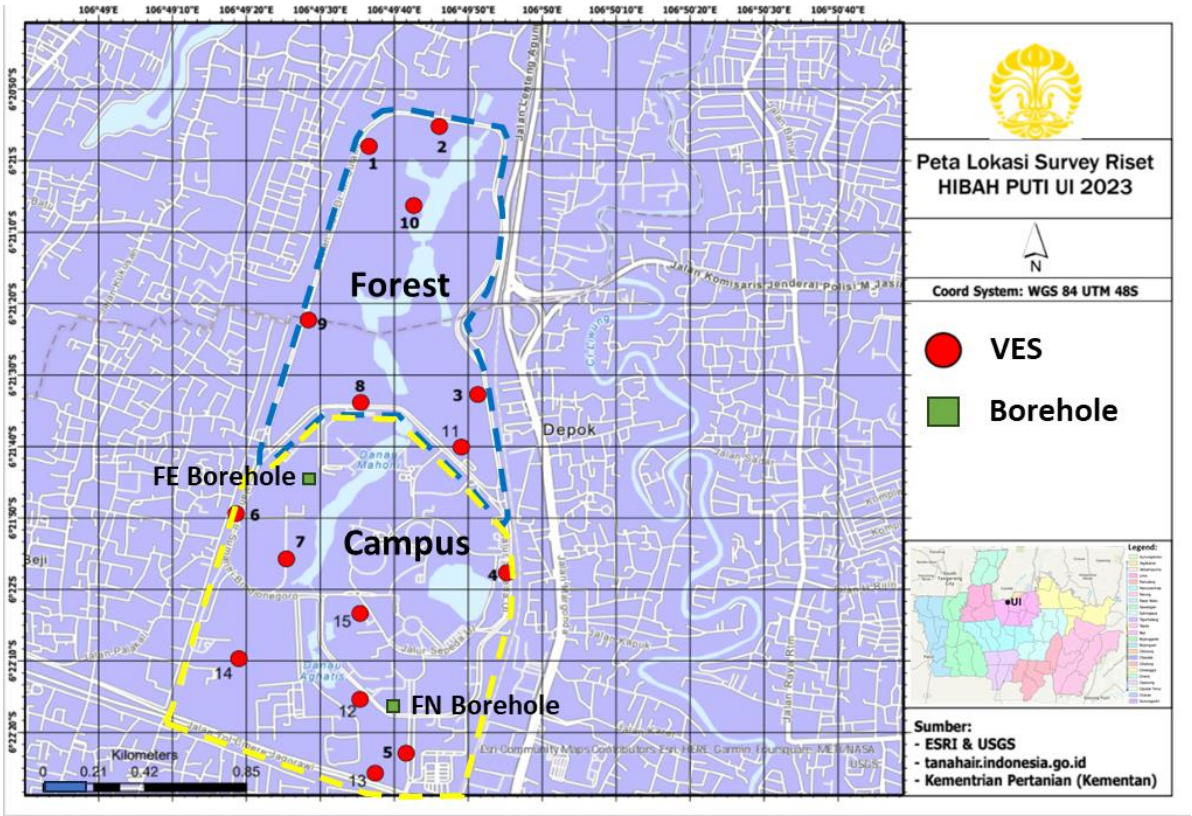

Figure 1. The study area is located in Universitas Indonesia (UI). Fifteen VES measurements (red dots) were performed to cover the forest area in the North and the Campus area in the South, shown by blue and yellow dotted lines. Two boreholes are available in the study area, located in the Faculty of Engineering (FE borehole) and the Faculty of Nursing (FN borehole). Green rectangulars depict the location of boreholes on the map.

FE and FN boreholes have a maximum depth of 30 m, respectively (Figure 2). They contain a similar lithology: sand, silt, and clay distributed at different depths. For the FE borehole, sand layers are at 9.5 m – 13 m, 16 m – 18 m, and 20 m – 29 m, silt layers are at 5.5 m – 9.5 m and 13 m – 16 m, and clay layers are at 0 m – 5.5 m, 18 m – 20 m, and 29 m – 30 m. For the FN borehole, sand layers are at 8 m – 12 m and 16 m – 24 m, silt layer is at 24 m – 30 m, and clay layer is at 0 m – 8 m and 12 m – 16 m.

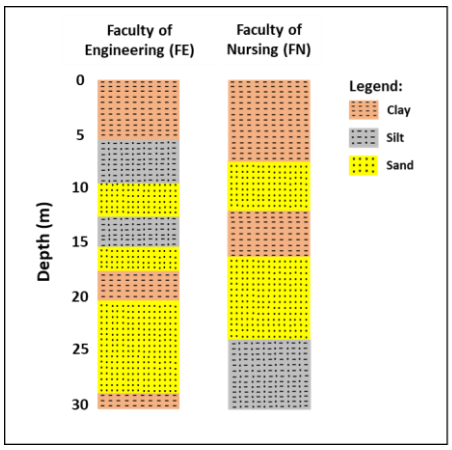

Figure 2. The lithology logs from FE and FN boreholes. The lithology type consists of sand, silt and clay. The location of boreholes in the study area can be seen in Figure 1. The correlation between boreholes is not conducted because the sediment age is unknown.

Sand layers are potential groundwater aquifers due to their higher interparticle porosity and permeability than silt and clay layers. Comparing sand layers in two boreholes indicates that the aquifers vary in thickness in the study area. FE borehole has thicker sand layers than in FN borehole. The lithology log will be used as guidance to interpret the lithology types from resistivity values obtained from VES measurements.

3. Methodology

3.1 Resistivity Method

The resistivity method is based on Ohm's law, which is performed by injecting electric current into the subsurface through current electrodes, whereas potential electrodes measure the potential difference generated between the current electrodes (Figure 3). Because current intensity is also recorded, it is possible to determine the apparent resistivity of the subsurface at the middle of potential electrodes (Telford et al., 1990), as shown by Equation 1.

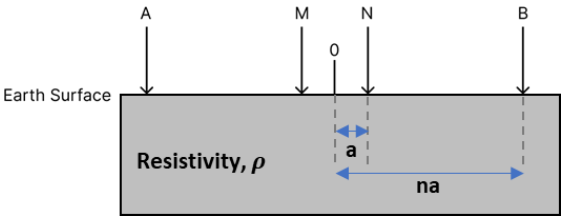

Figure 3. Schematic resistivity measurement in the field. Electrical current is injected through current electrodes (A and B), while the potential difference between current electrodes is measured by potential electrodes (M and N). a is half spacing between potential electrodes measured from midpoint (o), whereas n represents the number of half spacing increments between current electrodes. In VES measurement, n will be increased several times to resolve deeper subsurface layers.

$$\rho = k\frac{\Delta V}{I} \qquad (1)$$

where ρ is apparent resistivity of subsurface layers (Ωm), k is geometric factor of electrode configuration (m), ΔV represents potential difference between potential electrodes M and N (V) (Figure 3), and I is the current intensity injected into the subsurface by current electrodes A and B (A) (Figure 3). The geometric factor used in VES measurements is explained in the following sub-section.

3.2 VES Method

The VES method uses a Schlumberger array, where four electrodes (current and potential) are arranged between a fixed midpoint (Figure 3). The current electrodes (AB) are then moved outward to a new half spacing by a factor of n, while the potential electrodes (MN) remain with the same half spacing (Figure 3). The disadvantage of small MN spacing is that the signal can be relatively weak as AB spacing increases. Therefore, the MN spacing in the field also increases proportionately to the increasing MN spacing to better record the potential difference (ΔV in Equation 1) (Telford et al., 1990). It is important to note that the AB spacing is always larger than the MN spacing.

The outward movement of current electrodes provides better depth penetration than other array types, such as Wenner, where both current and potential electrodes are moved while maintaining the same spacing between them. The maximum distance between current electrodes in the Schlumberger array is obtained when (1) The measured potential difference becomes too small and/or (2) the space in which VES measurement is conducted does not allow for further outward movement of the current electrodes. The geometric factor of the Schlumberger array is shown below (Everett 2013).

$$k = (n-1)(n+1)\frac{\pi a}{2} \quad (2)$$

where k is geometric factor (m), a represents half spacing between potential electrodes (m), and n represents the number of half spacing increments between current electrodes (-). Hence, by substituting Equation 2 to 1, the apparent resistivity from VES method can be calculated using Equation 3 below.

$$\rho_a = (n-1)(n+1)\frac{\pi a}{2}\frac{\Delta V}{I} \quad (3)$$

3.3 Kriging Method

Kriging is a spatial interpolation technique using variogram analysis. It is based on the spatial autocorrelation of data points to estimate values at unmeasured locations by accounting for their spatial dependence and variability. Arslan (2012) used the Kriging method to generate predictive maps that interpolate groundwater salinity values at unsampled locations. Kriging is performed by calculating the experimental semivariogram, which indicates the correlation between data points shown as semivariance and distance vector, as shown by Equation 4.

$$\hat{\gamma}(h) = \frac{1}{2N}\sum_{i=1}^{N(h)}[z(x_i+h) - z(x_i)]^2 \quad (4)$$

where $\hat{\gamma}(h)$ is the estimated value of the semivariance for distance vector h, N is the number of pairs found at distance vector h, $z(x_i)$ is data point at location x_i, and $z(x_i+h)$ is other data points separated from $z(x_i)$ by distance vector h, x_i and x_i+h is the position of data points in two dimensions (Vijayakumar & Remadevi, 2006)

The performance of kriging prediction at unmeasured locations can be analysed using Mean Error (ME) and Root Mean Square Error (RMSE), as shown by Equations 5 and 6. Smaller ME and RSME mean more accurate predictions.

$$ME = \sum(Z_{i*} - Z_i) \quad (5)$$

$$RMSE = \sqrt{\frac{\sum(Z_{i*}-Z_i)^2}{n}} \quad (6)$$

Here, Zi is the predicted value, Zi$*$ is the observed value, and n is the number of observations. This study uses the Kriging method to interpolate aquifer thickness and depth of top aquifer distribution in the study area. This helps in the identification of potential aquifer zones and provides valuable insights into the heterogeneity of subsurface materials.

3.4 Survey Plan

VES survey is conducted in several steps. The first step involves creating a map of VES Lines and array directions by considering field conditions (i.e., roads, buildings, etc). The second step is preparing measurement tools, which include electrodes (current and potential), cables, batteries for power sources, GNSS for geospatial measurement, a laptop, and a main unit (Naniura hardware) for recording potential differences and current intensity. The last step is data collection in the

field by injecting electrical current into the subsurface using current electrodes and measuring potential differences using potential electrodes.

In this study, VES measurements have different half spacings of current and potential electrodes (a and na in Equations 2 and 3) (see also Figure 3). a values are varied from 0.25 m to 20 m, while the na values are between 0.5 m to 90 m depending on the space available at the measurement sites, as shown in Table 1. This leads to a variation of the maximum depth that can be resolved between measurement sites, which varies from 11.39 m to 61.89 m (Appendix 1). The measured VES data (current intensity and potential difference) is used to calculate apparent resistivity values using Equation 3, which are further interpreted using curve matching inversion technique to obtain thickness, depth, and true resistivity of subsurface layers using the IPI2WIN Software Package (Appendix 1). The RMS error during the interpretation is kept below 5 %.

Table 1. a and na values from all VES lines

Line	Range a	Range na
1	0.25-20 meter	0.50-90 meter
2	0.25-20 meter	0.50-90 meter
3	0.25-20 meter	0.50-90 meter
4	0.25-20 meter	0.50-90 meter
5	0.25-20 meter	0.50-90 meter
6	0.25-20 meter	0.50-90 meter
7	0.25-20 meter	0.50-90 meter
8	0.25-20 meter	0.50-90 meter
9	0.25-20 meter	0.50-90 meter
10	0.25-20 meter	0.50-90 meter
11	0.25-20 meter	0.50-75 meter
12	0.25-20 meter	0.50-90 meter
13	0.25-20 meter	0.50-90 meter
14	0.25-10 meter	0.50-50 meter
15	0.25-10 meter	0.50-50 meter

4. Rock Resistivity

The resistivity of shallow subsurface layers is mainly influenced by water content (Telford et al., 1990). Water is a conductive fluid. Therefore, the higher water content in the layers lowers their resistivity values. In addition, clay also attracts water in its matrix due to ion exchange. Each lithology has different water content and mineralogy, leading to a range of resistivity values that can overlap with other lithology types. This makes it challenging to distinguish lithology types based on their resistivity values alone. The resistivity values of various rocks and sediment are shown in Table 2.

Table 2. Rock and Fluid Resistivity Values (Telford et al., 1990)

Material	Resistivity
Air	0
Pyrite	0,01 - 100
Quartz	500 - 800.000
Calcite	$1x10^{12}$-$1x10^{13}$
Rock Salt	30 -$1x10^{13}$
Granite	200 – 100.000
Andesite)	1,7 x 10^2 – 45 x 10^4
Basalt	200 – 100.000
Limestones	500 – 10.000
Sandstones	200 – 8.000
Shales	20 – 2.000
Sand	1 – 1.0000
Clay	1 – 100
Ground Water	0.5 – 300
Sea Water	0.2
Magnetite (Magnetit)	0,01 – 1.000
Dry Gravel	600 – 10.000
Alluvium	10 – 800
Gravel	100 - 600

In this study, the target aquifer is sand layers, which have higher porosity and permeability than other lithology types in the study area, such as silt and clay. Understanding the thickness and distribution of aquifers is important in delineating potential aquifers in the study area. It is important to note that the resistivity values of aquifers can be different from Table 2 due to different water content and mineralogy (i.e., clay content). In addition, we

assume that temperature has a limited effect on the resistivity of shallow aquifers (< 90 m).

5. Result

5.1 Resistivity of Aquifers

We define a base case scenario by interpreting lithology types using true resistivity values obtained from curve-matching inversion for VES Line 5 (Figures 4A, B). The interpretation is guided by the information on lithology types from the FN borehole located a few metres from VES Line 5 (Figures 1, 2, and 4C). In addition, we also use rock resistivity values from the literature to help in the interpretation (Table 2). Note that the interpretation result cannot be validated because no borehole data (lithology types and resistivity log) is available at the site of VES Line 5.

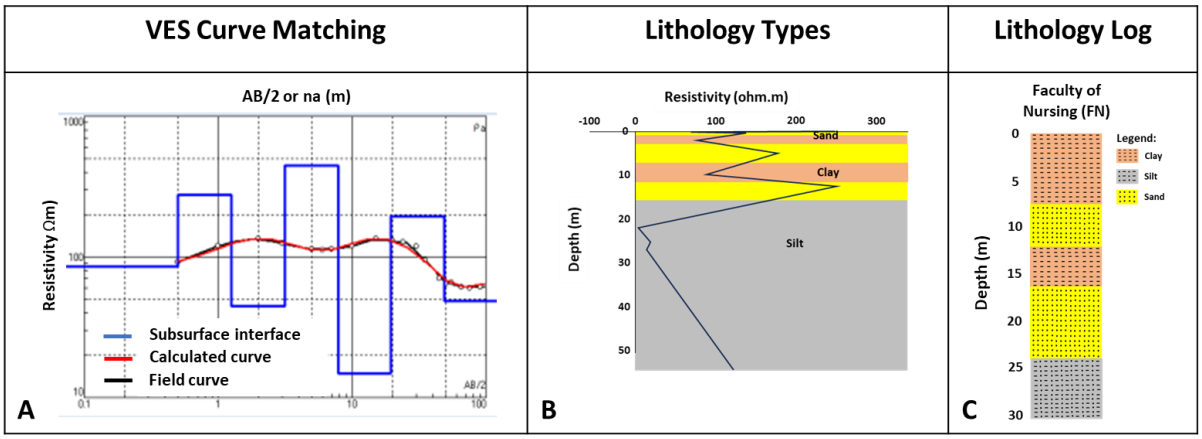

Figure 4. Analysis of measured VES data using curve matching inversion techniques (A). Resistivity values from VES Line 5 obtained from the inversion step represent the true resistivity of subsurface layers, interpreted to determine their respective lithology types (B). The lithology interpretation is guided by lithology log from FN borehole (C) and rock resistivity values from the literature (see also Table 2).

The result shows that the base case scenario has lithology types similar to those of the lithology log (Figures 4B, C). The true resistivity values and their representative lithology types from the base case scenario are then used as a basis for the identification of lithology types in other VES Lines (Appendix 1). A summary of resistivity values and their representative lithology types for all VES Lines are shown in Table 3.

Table 3. Interpretated lithology types and their resistivity ranges from the literature and VES.

Lithology Type	Literature (Telford, 1990)	VES
Clay	10-100 (Ωm)	3.68-110 (Ωm)
Sand	58.2-1048 (Ωm)	14.54-868 (Ωm)
Silt	20-97 (Ωm)	2.113-122.9 (Ωm)

The interpretation of lithology types indicates that the subsurface layers in the study area mainly contain three layers: sand, silt, and silt. Sand layers have resistivity values ranging from 14.54-868 Ωm, interpreted as aquifers. Silt layers have resistivity values from 2.113-122.9 Ωm, whereas clay layers have resistivity values ranging from 3.68-110 Ωm.

The aquifers are found in almost VES Lines, which mainly have resistivity values of less than 300 Ωm. A similar range of values is also shown in other studies (Damayanti, 2023; Ishaq, 2008). However, for several lines (L1, L7, L10, L12, L13, and L15), the aquifers have relatively high resistivity values (> 300 Ωm) (Table 4). No aquifers are found in L14 (Table 4).

Table 4. The resistivity, depth, and thickness of sand layers from all VES lines. The sand layers are interpreted as aquifers to host groundwater.

Line	Resistivity (Ohm.m)	Depth (m)	Thickness (m)	Lithology
L1	106-480	3.13–7.82	4.69	Sand
	288	19.4–48.5	29.1	Sand
L2	141.7	0.292–0.478	0.186	Sand
	114.1	1.114–1.931	0.817	Sand
	65.74-102	4.341–11.38	7.039	Sand
L3	75.92-110.4	0.5–3.125	2.625	Sand
	14.54-93.18	7.813–16.05	8.237	Sand
L4	80.91	7.813–19.53	11.717	Sand
L5	250.2	0-0.225	0.225	Sand
	139.4	0.341-0.373	0.032	Sand
	178.1	2.332-5.148	2.826	Sand
	133.5–251.9	10.16–15.54	5.38	Sand
L6	85.2-277	0.2–1.25	1.05	Sand
	194	19.5-48.8	29.3	Sand
L7	232.8-828.3	0-0.568	0.568	Sand
	540.3	0.967-2.116	1.149	Sand
	252.7	4.682-11.59	6.908	Sand
	970.4	15.86-17.1	1.24	Sand
L8	117-120	1.25-7.81	6.6	Sand
L9	149	0-0.648	0.648	Sand
	126.2	4.008-5.979	1.971	Sand
L10	442.9	1.521-3.022	1.501	Sand
L11	114.9	0-0.5	0.5	Sand
L12	337-868	1.09-4.85	3.76	Sand
L13	178.5-601.4	1.25-7.813	6.563	Sand
	230.1	19.53-48.83	29.3	Sand
L14	-	-	-	-
L15	151	0.5-1.25	0.75	Sand
	399	3.13-5.38	2.25	Sand
	342	12.5-19.5	7	Sand

5.2 Aquifers Distribution

The maps of isopach and depth of top aquifers are shown in Figures 5 and 6. These maps are generated using the Kriging method (Section III-3). The isopach map shows that aquifers thin towards the eastern part of the study area (up to 0.186 m) (Figure 5), whereas thicker aquifers are found towards the western part of the study area (up to 29.3 m) (Figure 5).

The map of top aquifers shows that aquifers can be found at shallow depths (min 0.5 m) almost in the entire study area (except for L14) (Table 4) (Figure 6). However, deeper top aquifer trend can also be observed towards the Northeast of the study area (up to 9.5 m) (Figure 6).

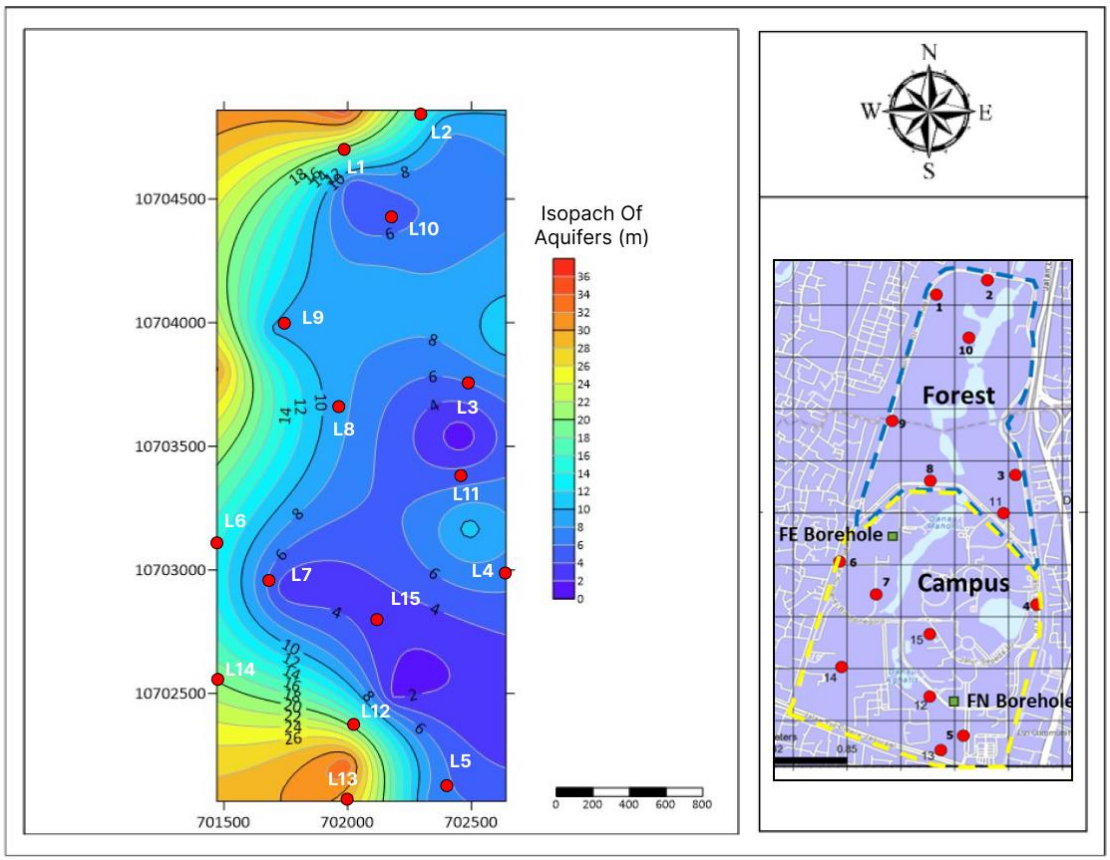

Figure 5. Isopach map of aquifers within the study area

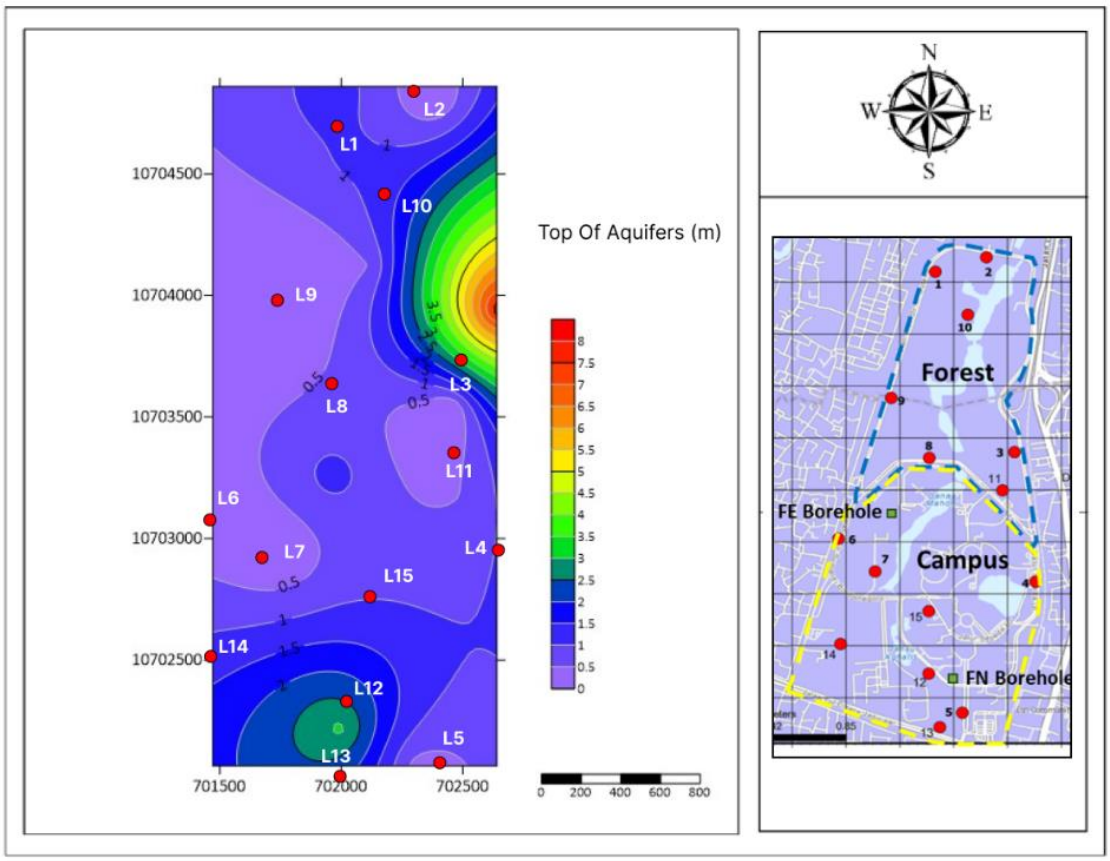

Figure 6. Top of aquifers within the study area

6. Discussion

This study uses Vertical Electrical Sounding (VES) with Schlumberger array to delineate the groundwater aquifers at UI area. The Schlumberger array is chosen to minimise noise generated from electrode movements and optimise the measurement time efficiency. In addition, the effect of shallow lateral variations in resistivity can be minimised as the position of potential electrodes is relatively fixed (Telford et al., 1990). The interpreted lithology from all VES Lines has layered stratigraphy, confirmed by the lithology log from boreholes. The result shows three distinct subsurface layers: sand, silt, and clay. The aquifer target is sand layers because they have relatively higher porosity and permeability than silt and clay. However, more studies need to be conducted to assess whether aquifers in different VES Lines are connected or part of a different system.

The aquifers are identified at shallow depths (< 50 m) and predominantly have resistivity values of less than 300 Ωm. However, in several lines (L1, L7, L10, L12, L13, and L15), the resistivity values reach up to 868 Ωm, which can occur due to several reasons: (1) Partial compaction occurs in the study area, leading to different pore fluid expulsion rates, eventually reaching the upper, less compacted aquifers. Consequently, some aquifers become less saturated, leading to higher resistivity values. (2) Sand aquifer in these VES Lines can be associated with local overbank deposits isolated by clay layers with lower porosity and permeability, hindering groundwater flow towards the deposits. As a result, they are mainly less saturated, leading to higher resistivity values. (3) The study area can also contain landfill sediments, which generally exhibit high resistivity anomalies (Ishaq, 2008)

7. Conclusion

This study has several conclusions: (1) The aquifers are found at shallow depths, which consist of sand intercalated with silt and clay. (2) The thicker aquifers are mainly distributed towards the western part of the study area (up to 29.3 m) and can be found at shallow depths (min 0.5 m)

Acknowledgement

We acknowledge the Hibah Publikasi Terindeks Internasional (PUTI) Q2 NOMOR: NKB-734/UN2.RST/HKP.05.00/2023 from Universitas Indonesia, which the corresponding author receives. The author would also like to thank the Department of Geoscience, which provides the resistivity measurement tools. In addition, we also appreciate Khoiru, Nanda, and the resistivity team that assisted in data acquisition.

References

Aizebeokhai, A. P., and O. A. Oyebanjo. 2013. “Application of Vertical Electrical Soundings to Characterize Aquifer Potential in Ota, Southwestern Nigeria.” Vol. 8(46):2077–85. doi: DOI: 10.5897/IJPS2013.4017.

Arslan, Hakan. 2012. “Spatial and Temporal Mapping of Groundwater Salinity Using Ordinary Kriging and Indicator Kriging: The Case of Bafra Plain, Turkey.” Agricultural Water Management 113:57–63. doi: https://doi.org/10.1016/j.agwat.2012.06.015.

Coker, J. O. 2012. “Vertical Electrical Sounding (VES) Methods to Delineate Potential Groundwater Aquifers in Akobo Area, Ibadan, South-Western, Nigeria.” (Vol.4(2)):35–42. doi: https://doi.org/10.5897/JGMR11.014.

Damayanti, N. T. 2023. “Identifikasi Zona Jenuh Air Dengan Metode Resistivity Vertical Electrical Sounding (VES) Di Lokasi Pembukaan Tambang PT. Mandiri IntiPerkasa, Kalimantan Utara.” Master Thesis, Universitas Indonesia, Depok.

Dzakiya, N., M. F. Zakaria, D. E. Setiawan, and R. B. Laksmana. 2021. “Study of Groundwater Types Using the Vertical Electrical Sounding (VES) Method in the

'Martani Field' Ngemplak District of Yogyakarta." 5(1).

Everett, Mark E. 2013. Near-Surface Applied Geophysics. Cambridge University Press.

Hadian, M. S. D., U. Mardiana, O. Abdurahman, and M. I. Iman. 2006. "Sebaran Akuifer Dan Pola Aliran Air Tanah Di Kecamatan Batuceper Dan Kecamatan Benda Kota Tangerang, Provinsi Banten." Jurnal Geologi Indonesia 1(3).

Hamzah, Umar, Abdul Rahim Samsudin, and Edna Pilis Malim. 2007. "Groundwater Investigation in Kuala Selangor Using Vertical Electrical Sounding (VES) Surveys." Environmental Geology 51(8):1349–59. doi: 10.1007/s00254-006-0433-8.

Ishaq, Z. M. 2008. "Studi resistivitas dan gravitasi untuk investigasi akuifer air bawah-tanah di kampus UI Depok." Master Thesis, Universitas Indonesia, Depok.

Koesuma, A., and A. Aldi. 2022. "Identification of Groundwater Depth in the Northern Sukoharjo Regency Using Vertical Electrical Sounding (VES) Method to Overcome Agricultural Irrigation Drought." (986 012079). doi: doi:10.1088/1755-1315/986/1/012079.

Lab Mekanika Tanah. 2008. Borehole Logs. Kampus UI: Universita Indonesia.

Maulana, R. 2022. "Sukoharjo Regency Using VES Method as a Means of Irigation of Agricultural Land." (989 012003). doi: doi:10.1088/1755-1315/989/1/012003.

Muzakki, Y., W. Lestari, and M. Fajar. 2021. "Pemodelan akuifer air tanah menggunakan geolistrik resistivitas VES di kabupaten sorong, provinsi papua barat." Jurnal Geosaintek 7(3). doi: http://dx.doi.org/10.12962/j25023659.v7i3.8789.

Nuraini, Fera, ade suryani siregar, Dzirana Sekar Arum, and Suhendra. 2022. "Pendugaan Air Tanah Menggunakan Metode Tahanan Jenis Di Kelurahan Kandang Limun, Kota Bengkulu." Newton-Maxwell Journal of Physics 3(2):65–70. doi: 10.33369/nmj.v3i2.24078.

Rizqulloh, M. R., and A. Riyanto. 2020. "Analysis distribution of brittlness index, modulus young, modulus bulk, and poisson's ratio using the integration of refraction seismic method and MASW case study of Fasilkom UI's new building." Tugas Akhir, Universitas Indonesia, Depok.

Sholichin, M., and T. B. Prayogo. 2019. "Field Identification of Groundwater Potential Zone by VES Method in South Malang, Indonesia." 10(02):999–1009.

Syifaurrohman, Y., W. Utama, W. Lestari, and T. M. A. Surya. 2018. "Distribusi Sebaran Aquifer Air Tanah Menggunakan Data Resistivitas Metode Vertical Electrical Sounding (VES) Konfiguras Schlumberger (Studi Kasus Kabupaten Palu, Provinsi Sulawesi Tengah)." 4(2).

Telford, W., L. Geldart, and R. Sheriff. 1990. Applied Geophysics (2nd Ed.). Cambridge: Cambridge University Press.

Wahab, Shafiqullah, Hakim Saibi, and Hideki Mizunaga. 2021. "Groundwater Aquifer Detection Using the Electrical Resistivity Method at Ito Campus, Kyushu University (Fukuoka, Japan)." Geoscience Letters 8(1):15. doi: 10.1186/s40562-021-00188-6.

APPENDIX 1
True Resistivity Values of Subsurface Layers and Their Interpreted Lithology Types for All VES Lines

Line	Layer	Depth (m)	Lithology	Resistivity (Ωm)
1	1	0 – 0.2	Clay	61.4
	2	0.2 – 0.5	Clay	61.4
	3	0.5 – 1.25	Clay	78.2
	4	1.25 – 3.13	Clay	78.2
	5	3.13 – 3.88	Sand	480
	6	3.88 – 5.01	Sand	480
	7	5.01– 7.82	Sand	106
	8	7.82 – 12.5	Silt	6.01
	9	12.5 – 15.3	Silt	6.01
	10	15.3 – 19.4	Silt	6.01
	11	19.4 – 48.5	Sand	288

Line	Layer	Depth (m)	Lithology	Resistivity (Ωm)
2	1	0 – 0.2921	Clay	50.06
	2	0.2921 – 0.4776	Sand	141.7
	3	0.4776– 0.7706	Clay	12.9
	4	0.7706 – 1.114	Clay	23.44
	5	1.114 – 1.931	Sand	114.1
	6	1.931– 2.641	Clay	30.38
	7	2.641– 4.341	Clay	15.97
	8	4.341– 9.501	Sand	102
	9	9.501– 11.38	Sand	65.74
	10	11.38 – 18.12	Silt	9.538
	11	18.12 – 22.07	Silt	22.89
	12	22.07 – 55.4	Silt	36.78

Line	Layer	Depth (m)	Lithology	Resistivity (Ωm)
3	1	0 – 0.5	Clay	44.32
	2	0.5– 1.25	Sand	75.92
	3	1.25 – 3.125	Sand	110.4
	4	3.125 – 7.813	Clay	34.42
	5	7.813 – 12.5	Sand	93.18
	6	12.5 – 16.05	Sand	14.54
	7	16.05 – 19.53	Silt	14.54
	8	19.53 – 31.25	Silt	29.47
	9	31.25 – 48.83	Silt	29.47

Line	Layer	Depth (m)	Lithology	Resistivity (Ωm)
4	1	0 – 0.2	Clay	68.22
	2	0.2 – 0.5	Clay	68.22
	3	0.5 – 1.25	Clay	56.83
	4	1.25 – 3.125	Clay	58.46
	5	3.125 – 7.813	Clay	30.96
	6	7.813 – 19.53	Sand	80.91
	7	19.53 – 31.25	Silt	10.14
	8	31.25 – 48.83	Silt	10.14

Line	Layer	Depth (m)	Lithology	Resistivity (Ωm)
5	1	0 – 0.225	Sand	250.2
	2	0.255 – 0.3406	Clay	72.62
	3	0.3406 – 0.3726	Sand	139.4
	4	0.3726 – 2.332	Clay	76.84
	5	2.332 – 5.148	Sand	178.1
	6	5.148 –10.16	Clay	89.23
	7	10.16 –12.62	Sand	251.9
	8	12.62 –15.54	Sand	133.5
	9	15.54 – 21.85	Silt	7.445
	10	21.85 – 25.31	Silt	18.85
	11	25.31 – 27.79	Silt	15.52
	12	27.79 – 54.59	Silt	122.9

Line	Layer	Depth (m)	Lithology	Resistivity (Ωm)
6	1	0 – 0.2	Clay	85.2 (Overlapping)
	2	0.2 – 0.5	Sand	85.2
	3	0.5 – 1.25	Sand	277
	4	1.25– 3.13	Clay	44.7
	5	3.13 – 7.82	Clay	44.7
	6	7.82 – 12.5	Silt	14.9
	7	12.5 – 19.5	Silt	14.9
	8	19.5 – 31.2	Sand	194
	9	31.2 – 48.8	Sand	194

Line	Layer	Depth (m)	Lithology	Resistivity (Ωm)
7	1	0 – 0.0858	Sand	828.3
	2	0.0858 – 0.5675	Sand	232.8
	3	0.5675 – 0.9668	Clay	32.25
	4	0.9668 – 2.116	Sand	540.3
	5	2.116 – 2.477	Clay	26.09
	6	2.477 – 4.682	Clay	44.43
	7	4.682 – 11.59	Sand	252.7
	8	11.59 – 15.86	Silt	13.79
	9	15.86 – 17.1	Sand	970.4
	10	17.1 – 25.78	Silt	7.568
	11	25.78 – 26.59	Silt	38.21
	12	26.59– 59	Silt	2.585

Line	Layer	Depth (m)	Lithology	Resistivity (Ωm)
8	1	0 – 0.5	Clay	70.4
	2	0.5– 1.25	Clay	85.6
	3	1.25 – 2	Sand	117
	4	2 – 3.13	Sand	117
	5	3.13 – 7.81	Sand	120
	6	7.81 – 12.5	Clay	86.8
	7	12.5 – 19.5	Clay	86.8
	8	19.5 – 30.1	Silt	36.7
	9	30.1 – 48.8	Silt	34.2

Line	Layer	Depth (m)	Lithology	Resistivity (Ωm)
9	1	0 – 0.648	Sand	149
	2	0.648 – 0.2223	Clay	81.92
	3	0.2223 – 0.591	Clay	46.4
	4	0.591 – 0.6272	Clay	4.939
	5	0.6272 – 1.127	Clay	65.33
	6	1.127 – 4.008	Clay	38.77
	7	4.008 – 5.979	Sand	126.2
	8	5.979 – 7.728	Silt	12.86
	9	7.728 – 18.9	Silt	54.02
	10	18.9 – 20.43	Silt	2.113
	11	20.43 – 30.97	Silt	23.44
	12	30.97 – 55.42	Silt	51.11

Line	Layer	Depth (m)	Lithology	Resistivity (Ωm)
10	1	0 – 0.4485	Clay	36.92
	2	0.4485 – 1.521	Clay	71.92
	3	1.521– 3.022	Sand	442.9
	4	3.022 – 9.639	Clay	30.72
	5	9.639 – 26.63	Clay	53.45
	6	26.63 – 40.63	Silt	4.97
	7	40.63 – 61.89	Silt	12.52

Line	Layer	Depth (m)	Lithology	Resistivity (Ωm)
11	1	0 – 0.2	Sand	114.9
	2	0.2– 0.5	Sand	114.9
	3	0.5 – 0.8	Clay	78.65
	4	0.8 – 0.98	Clay	12.9
	5	0.98 – 1.25	Clay	12.9

	6	1.25 – 3.125	Clay	27.65
	7	3.125 – 7.813	Clay	30.53
	8	7.813 – 19.53	Silt	26.5
	9	19.53 – 31.25	Silt	27.65
	10	31.25 – 48.83	Silt	27.65

Line	Layer	Depth (m)	Lithology	Resistivity (Ωm)
12	1	0 – 0.189	Clay	3.68
	2	0.189 – 0.246	Clay	21.6
	3	0.246 – 0.475	Clay	14.1
	4	0.475 – 1.09	Clay	3.99
	5	1.09 – 1.42	Sand	337
	6	1.42 – 1.97	Sand	868
	7	1.97 – 2.79	Sand	868
	8	2.79 – 4.85	Sand	801
	9	4.85 – 7.76	Silt	48.7
	10	7.76 – 12.1	Silt	48.7
	11	12.1 – 30.3	Silt	17.8

Line	Layer	Depth (m)	Lithology	Resistivity (Ωm)
13	1	0 – 0.2	Clay	26.94
	2	0.2 – 0.5	Clay	26.94
	3	0.5 – 0.8	Clay	48.65
	4	0.8 – 1.25	Clay	48.65
	5	1.25 – 3.125	Sand	601.4
	6	3.125 – 7.813	Sand	178.5
	7	7.813 – 19.53	Silt	67.33
	8	19.53 – 48.83	Sand	230.1

Line	Layer	Depth (m)	Lithology	Resistivity (Ωm)
14	1	0 – 0.2	Clay	66.93
	2	0.2 – 0.5	Clay	66.93
	3	0.5 – 1.25	Clay	86.87
	4	1.25 – 3.125	Clay	32.15
	5	3.125 – 7.813	Clay	34.07
	6	7.813 – 12.5	Clay	25.71
	7	12.5 – 19.53	Clay	29.35
	8	19.53 – 31.25	Clay	72.4
	9	31.25 – 48.83	Silt	11.52

Line	Layer	Depth (m)	Lithology	Resistivity (Ωm)
15	1	0 – 0.2	Clay	94
	2	0.2 – 0.5	Clay	94
	3	0.5 – 1.25	Sand	151
	4	1.25 – 2	Clay	110
	5	2 – 3.13	Clay	110
	6	3.13 – 5.38	Sand	399
	7	5.38 – 6.36	Silt	46.6
	8	6.36 – 7.82	Silt	46.6
	9	7.82 – 12.5	Silt	33.7
	10	12.5 – 19.5	Sand	342